Phase transitions with infinitely many absorbing states in complex networks

Renan S. Sander,[1] Silvio C. Ferreira,[1,*] and Romualdo Pastor-Satorras[2]
[1]*Departamento de Física, Universidade Federal de Viçosa, 36571-000 Viçosa, Minais Gerais, Brazil*
[2]*Departament de Física i Enginyeria Nuclear, Universitat Politècnica de Catalunya, Campus Nord B4, 08034 Barcelona, Spain*
(Received 28 September 2012; published 27 February 2013)

We investigate the properties of the threshold contact process (TCP), a process showing an absorbing-state phase transition with infinitely many absorbing states, on random complex networks. The finite-size scaling exponents characterizing the transition are obtained in a heterogeneous mean-field (HMF) approximation and compared with extensive simulations, particularly in the case of heterogeneous scale-free networks. We observe that the TCP exhibits the same critical properties as the contact process, which undergoes an absorbing-state phase transition to a single absorbing state. The accordance among the critical exponents of different models and networks leads to conjecture that the critical behavior of the contact process in a HMF theory is a universal feature of absorbing-state phase transitions in complex networks, depending only on the locality of the interactions and independent of the number of absorbing states. The conditions for the applicability of the conjecture are discussed considering a parallel with the susceptible-infected-susceptible epidemic spreading model, which in fact belongs to a different universality class in complex networks.

DOI: 10.1103/PhysRevE.87.022820 PACS number(s): 89.75.Hc, 05.70.Jk, 05.10.Gg, 64.60.an

I. INTRODUCTION

The role of the effects of a disordered substrate on the behavior of dynamical processes has attracted the attention of the statistical physics community for a long time [1,2]. The interest in this issue has been enhanced by the recent realization that the substrate of many relevant dynamical processes can be represented in terms of a complex network [3–5]. This realization has led to a renewed scientific effort emphasizing the effects of the disordered topology inherent to the underlying network [6,7]. In this context, it has been shown that highly heterogeneous contact patterns, characterized by a degree distribution $P(k)$ (probability that an element or vertex in the network is connected to other k vertices) showing a heavy-tailed form can have a very strong impact on processes such as epidemic spreading [8–10], percolation [11,12], or synchronization [13].

Among the different dynamical processes considered in networks, an important role has been played by the class of processes with absorbing states [14,15]. Absorbing states are configurations of the system in which the dynamics becomes trapped forever and that usually imply the presence of absorbing-state phase transitions (APTs) between an active phase and the absorbing configurations. The simplest model exhibiting an APT is the contact process (CP) [16], where particles lying on a lattice or network undergo spontaneous annihilation and catalytic creation. A creation event involves a pair of empty and occupied nodes and is controlled by a rate λ. The CP undergoes a continuous APT at a critical point λ_c, separating an absorbing phase with all sites empty from an active one with a nonzero order parameter ϕ, defined as the average density of particles at the steady state. The ensuing APT is characterized in terms of a set of critical exponents that define the so-called directed percolation (DP) universality class [15]. The theoretical analysis of the CP in networks [17–19], based on the heterogeneous mean-field (HMF) theory [6,7], has shown the presence of an APT in which the scaling of the relevant critical quantities with network size presents very strong corrections to scaling in scale-free (SF) networks with a heterogeneous degree distribution given by a power law form, $P(k) \sim k^{-\gamma}$ [3]. These corrections to scaling, albeit very large, have been observed in large-scale numerical simulations [20].

While simple models such as the CP are characterized by a unique absorbing state devoid of all particles, other relevant systems present multiple absorbing configurations [21]. Examples of those range from models of forest fires [22] to self-organized critical sand piles [23]. A basic model presenting an APT with multiple absorbing states is the pair contact process (PCP), where a pair of occupied neighbors annihilates with probability p and creates a new particle in one nearest neighbor (NN) of the pair with probability $1 - p$ [24]. Any configuration with only isolated particles is an absorbing state, which implies that the PCP has infinitely many absorbing configurations in the thermodynamic limit. On lattices, the PCP belongs to the DP universality class [15].

In the field of complex networks, dynamical systems with many absorbing states have been used to investigate self-organized criticality and avalanches [25–27], while the analysis of the ensuing APT is limited to a few works [28,29]. The HMF analysis of the forest fire model in heterogeneous networks yielded critical exponents equal to those obtained for the susceptible-infected-susceptible epidemic model in the same approach [28]. A finite-size scaling [30] analysis of the PCP was performed for homogeneous networks [29], but using very limited sizes, which do not allow to extract reliable conclusions about the model's universality class.

In this work, we present and analyze a model possessing an APT with many absorbing states, which is amenable to analytical calculations based on the HMF formalism and large-scale numerical simulations. The model, which we call the threshold contact process (TCP), is inspired by the PCP, with the peculiarity that the *fermionic* constraint of single occupation of vertices is relaxed to allow double occupation. This modification hugely reduces the computer algorithmic

*silviojr@ufv.br

complexity and allows us to perform a standard HMF analysis [6,7,31]. We show that the behavior of the TCP at the HMF level is the same of the CP, a fact that we confirm by means of extensive numerical simulations based on the quasistationary state method [19,20,32]. We thus conclude that, despite the nonfermionic nature of the TCP, it extends to complex networks the fundamental inclusion of the PCP in the universality class of the contact process.

We have organized our paper as follows: In Sec. II we present a brief overview of the properties of the CP on complex networks. Section III is devoted to describing the TCP model. A HMF theory and a homogeneous pair approximation for the TCP are developed in Sec. IV. The simulation methods and numerical procedures used are described in Sec. V, where we also present a check of the HMF theory by means of numerical simulations on annealed networks. Simulations on real quenched networks are presented in Sec. VI, where we compare them with the HMF theory predictions. Finally, we draw our concluding remarks in Sec. VII.

II. THE CONTACT PROCESS ON NETWORKS

The CP dynamics on networks is defined as follows [33]: Every node can be either occupied or empty. Occupied nodes become empty at a rate of 1, while empty sites become occupied at a rate $\lambda n/k$, where k is the number of NNs of the node (the node's degree), and n is the number of occupied nodes among the NNs.

The properties of the CP dynamics on heterogeneous networks have been analytically investigated within the framework of the HMF theory [17–19,33], an extension of the standard mean-field theory taking into account the network heterogeneity. The HMF theory assumes that the vertex degree is the only relevant quantity, substitutes the topological structure of the network by an annealed form [6,7], and neglects all dynamical correlations between vertices. In HMF theory, focus is placed on the partial densities of particles in vertices of degree k, denoted by ϕ_k, which satisfy the rate equation [33]

$$\frac{d\phi_k}{dt} = -\phi_k + \lambda k[1-\phi_k]\sum_{k'}\frac{P(k'|k)\phi_{k'}}{k'}. \tag{1}$$

The quantity $P(k'|k)$ is a measure of the degree correlations [4], defined as the conditional probability that a vertex of degree k is connected to a vertex of degree k' [34]. The solution of this equation in the stationary limit leads to an APT located at the critical point $\lambda_c = 1$, irrespective of the degree correlations in the network. For degree uncorrelated networks, in which $P(k'|k) = k'P(k')/\langle k\rangle$ [4], a complete solution can be worked out [33], giving an order parameter defined as the average particle density that close to the critical point scales as $\phi = \sum_k P(k)\phi_k \sim (\lambda-\lambda_c)^{\beta}$, a characteristic time scaling as $\tau \sim (\lambda-\lambda_c)^{-\nu}$, and a decay of the particle density at the critical point $\phi_c(t) \sim t^{-\delta}$. In SF networks with degree distribution $P(k) \sim k^{-\gamma}$, one has $\beta = \delta = \max\{1/(\gamma-2),1\}$, while $\nu = 1$ for any γ.

These critical exponents, depending on the degree distribution, are valid in the thermodynamic limit of an infinite network. In finite systems, however, the transition to the absorbing state is better characterized in terms of a finite-size scaling (FSS) analysis [30]. In Refs. [17,19,35] such a theory was developed, exploiting a mapping of the CP in the low density regime to a one-step process. Within this approximation, one can build the equation for the probability distribution $\bar{P}_n$ of observing n active particles in the steady state, which in the thermodynamic limits takes a scaling form given by [19]

$$\bar{P}_n = \frac{1}{\sqrt{\Omega}} f\left(\frac{n}{\sqrt{\Omega}}\right), \tag{2}$$

where f is a scaling function normalized as $\int_0^\infty f(x)dx = 1$, $\Omega = N/g$, and $g = \langle k^2\rangle/\langle k\rangle^2$. The critical density and characteristic time follow directly from this distribution [19] and are given by

$$\bar{\phi} \sim (Ng)^{-1/2} \quad \text{and} \quad \tau \sim (N/g)^{1/2}. \tag{3}$$

For a power law degree distribution, the factor g diverges with the degree cutoff k_c (the largest degree present in the network) as $g \sim k_c^{3-\gamma}$ for $\gamma < 3$ and becomes constant (logarithmic) for $\gamma > 3$ ($\gamma = 3$) [36]. For a general cutoff scaling as $k_c \sim N^{1/\omega}$, the scaling laws

$$\bar{\phi} \sim N^{-\hat{\nu}} \quad \text{and} \quad \tau \sim N^{\hat{\alpha}} \tag{4}$$

ensue in the limit $N \to \infty$, with associated critical exponents [19]

$$\hat{\nu} = \frac{1}{2} + \max\left(\frac{3-\gamma}{2\omega},0\right), \quad \hat{\alpha} = \frac{1}{2} - \max\left(\frac{3-\gamma}{2\omega},0\right). \tag{5}$$

These exponents, which define what we can call the CP universality class at the HMF level (the CP-HMF class), have been proved to provide a correct description of the CP in networks by means of large-scale numerical simulations [20], corroborating thus the validity of the description of the CP on networks in terms of the HMF theory.

III. THE THRESHOLD CONTACT PROCESS

One of the simplest models exhibiting a transition to infinitely many absorbing states is the PCP [24]. An optimized computer simulation of PCP near the critical point (low density of active sites) requires the maintenance of an updated list containing the coordinates of all active pairs. This task becomes computationally inefficient when the model is implemented on an arbitrary graph, more specifically during the annihilation events when the involved pair and all the corresponding active links must be removed from the list. Kockelkoren and Chaté [37] had already realized that the fermionic constraint can be counterproductive in lattices due to algorithmic complexity and, more importantly, due to strong deviations from scaling originating from this restriction. For this reason, we consider a modification of the PCP that we call the TCP, which is defined by the following rules: Nodes can be occupied by 0, 1, or 2 particles (i.e., they can have an occupation number $\sigma_i = 0,1,2$). Particles in a doubly occupied node can be either annihilated at rate 1 or can create an offspring particle in a randomly chosen NN at rate λ. The creation event actually takes place only if the selected NN is empty or singly occupied. Because empty and singly occupied nodes do not react, any

configuration devoid of doubly occupied sites is an absorbing state. Singly occupied sites do, however, play a fundamental role, since they form a backbone of connected vertices through which activity can spread. The TCP can be easily generalized to higher thresholds (maximum occupation number), $h > 2$.

The computer implementation of TCP in an arbitrary graph can be done with the following scheme: At each time step, an active (doubly occupied) vertex j is randomly chosen and time is updated as $t \to t + \Delta t$, where $\Delta t = 1/[(1+\lambda)n(t)]$ and $n(t)$ is the number of active vertices at time t. With probability $p = 1/(1+\lambda)$, both particles of the selected vertex are annihilated, producing an empty vertex. With the complementary probability $1 - p = \lambda/(1+\lambda)$, one of the k neighbors of j is randomly selected and, if empty or singly occupied, receives a new particle; otherwise, nothing happens and the simulation proceeds to the next time step. Although we have checked numerically that the TCP belongs to the DP class in regular d-dimensional lattices (to be reported elsewhere), in the following we consider its behavior in complex networks.

IV. MEAN-FIELD ANALYSIS

A. Homogeneous mean-field theory

In homogeneous substrates such as a regular lattice, all nodes are equivalent and thus the equations of motion are the same for all of them. Letting $\Pi(\sigma_1,\ldots,\sigma_l)$ be the probability that a cluster of l vertices has the configuration $\{\sigma_1 \ldots \sigma_l\}$, we can find the following exact equations of motion for single sites in the TCP dynamics:

$$\frac{d\Pi(2)}{dt} = -\Pi(2) + \lambda\Pi(1,2), \tag{6}$$

$$\frac{d\Pi(1)}{dt} = \lambda[\Pi(0,2) - \Pi(1,2)]. \tag{7}$$

The equations for single nodes depend on pairs, those for pairs depend on triplets (as we will see below), and so forth. An approximate solution can be obtained by breaking this hierarchy of equations by means of some closure condition. Thus, in the simplest one-site approximation, the correlation between pairs is neglected, resulting in $\Pi(\sigma,\sigma') \approx \Pi(\sigma)\Pi(\sigma')$ [14]. Equations (6) and (7) in this one-site approximation become

$$\frac{d\phi}{dt} = -\phi + \lambda\rho\phi, \tag{8}$$

$$\frac{d\rho}{dt} = \lambda\phi(1 - \phi - 2\rho), \tag{9}$$

where we have defined $\phi = \Pi(2)$, $\rho = \Pi(1)$, and obviously $\Pi(0) = 1 - \rho - \phi$. In the stationary regime, Eqs. (8) and (9) yield $\rho = 1/\lambda$ and $\phi = (\lambda - 2)/\lambda$. We can therefore identify the critical point $\lambda_c = 2$ and the DP mean-field exponent $\beta = 1$ [14]. One can easily verify that the characteristic time τ scales with the DP mean-field exponent, $\tau \sim (\lambda - \lambda_c)^{-1}$, while the density of active sites decays with time at criticality as $\phi_c \sim t^{-1}$.

For the case of the CP, it has been shown that a homogeneous pair approximation (HPA) [38], considering the hierarchy of equations up to second order, yields better estimates of the critical point even in the realistic case of heterogeneous networks [20,39]. We can also follow this HPA approach for the TCP. First, we observe that in the stationary regime Eqs. (6) and (7) give $\Pi(2,0) = \Pi(2,1) = \phi/\lambda$. Moreover, using the normalization condition $\Pi(0,2) + \Pi(1,2) + \Pi(2,2) = \Pi(2)$, we have $\Pi(2,2) = 1 - 2\phi/\lambda$. The equations for the remaining independent pairs are

$$\frac{d\Pi(0,0)}{dt} = 2\Pi(2,0) - 2\frac{q-1}{q}\lambda\Pi(0,0,2), \tag{10}$$

$$\frac{d\Pi(0,1)}{dt} = \lambda\frac{q-1}{q}[\Pi(0,0,2) - \Pi(0,1,2)], \tag{11}$$

$$\frac{d\Pi(1,1)}{dt} = 2\lambda\frac{q-1}{q}[\Pi(1,0,2) - \Pi(1,1,2)]. \tag{12}$$

Here q is the number of NNs of a vertex, which we assume to be constant for all vertices in this homogeneous approach. Furthermore, since homogeneity implies $\Pi(\sigma,\sigma') = \Pi(\sigma',\sigma)$, the evolution of all pair is determined given Eqs. (10)–(12).

Up to this point, all pair motion equations are exact. Now, we perform the pair approximation [38]

$$\Pi(\sigma,\sigma',\sigma'') \approx \frac{\Pi(\sigma,\sigma')\Pi(\sigma',\sigma'')}{\Pi(\sigma')}, \tag{13}$$

which, after applying normalization and symmetry conditions, leads to the following nonlinear equations for the stationary state:

$$\rho - \frac{\phi}{\lambda} = \frac{q}{\lambda(q-1)}\frac{\rho(1-\phi)}{1-\rho-\phi}, \tag{14}$$

$$\rho = 1 - \frac{q}{\lambda(q-1)} - \frac{\phi}{\lambda}\left[\lambda + 1 - \frac{q}{q-1}\right]. \tag{15}$$

Solving Eqs. (14) and (15) we obtain

$$\phi = \frac{\lambda - \lambda_c(q)}{\lambda - \lambda_c(q) + 2}, \tag{16}$$

where the critical point for general q is given by

$$\lambda_c(q) = \frac{2q}{q-1}. \tag{17}$$

In Sec. V we show that this result fits well the critical point obtained from computer simulations of TCP on networks.

B. Heterogeneous mean-field theory

Application of HMF to the TCP in heterogeneous networks follows the steps performed for the CP. In the heterogeneous case, we differentiate the functions ρ and ϕ according to degree, defining ϕ_k and ρ_k as the probability that a vertex of degree k is doubly or simply occupied, respectively. The rate equations (8) and (9) are thus simply modified within the approximation, now taking the form

$$\frac{d\phi_k}{dt} = -\phi_k + \lambda k\rho_k\Theta_k, \tag{18}$$

$$\frac{d\rho_k}{dt} = \lambda k(1 - 2\rho_k - \phi_k)\Theta_k, \tag{19}$$

where

$$\Theta_k = \sum_{k'} \frac{P(k'|k)\phi_{k'}}{k'} \tag{20}$$

is the probability that a vertex of degree k receives a particle from an active NN. As in the CP, the factor $1/k'$ accounts

for the random choice of the target neighbor for offspring creation from a vertex of degree k'. In the case of degree uncorrelated networks, we are led to the simplified coupling factor $\Theta_k \equiv \Theta = \sum_k \phi_k P(k)/\langle k\rangle \equiv \phi/\langle k\rangle$, independent of k.

In order to solve Eqs. (18) and (19), we notice that ϕ_k gives the order parameter $\phi = \sum_k P(k)\phi_k$ in the APT. The density $\rho = \sum_k P(k)\rho_k$ is a noncritical field coupled to the order parameter that goes to a finite value at the steady state even at the critical point or in the subcritical phase. We thus assume that it will reach its steady state in a way faster than ϕ. We have checked that this assumption is compatible with our numerical simulations (see Fig. 2). We thus proceed to perform a quasistatic approximation [40], imposing $\dot{\rho}_k \simeq 0$ in Eq. (19) to obtain

$$\rho_k \simeq \frac{1-\phi_k}{2}, \tag{21}$$

which, upon substitution into Eq. (18), leads to the equation

$$\frac{d\phi_k}{dt} \simeq -\phi_k + \frac{\lambda}{2}k(1-\phi_k)\Theta_k, \tag{22}$$

that holds for long times.

Equation (22) is exactly the same HMF rate equation obtained for the order parameter of the CP on heterogeneous networks [see Eq. (1)], with an effective creation rate $\lambda' = \lambda/2$. Therefore, we can exploit all results presented in Sec. II: For an infinite network size, the TCP will undergo a continuous APT at a critical $\lambda_c = 2$, independently of the connectivity pattern of the network. Under the additional simplification of degree uncorrelated networks, we recover the critical behavior $\phi \sim (\lambda - \lambda_c)^\beta$ with $\beta = \max\{1/(\gamma-2), 1\}$, while the characteristic time diverges as $\tau \sim |\lambda - \lambda_c|^{-1}$. At the critical point, the order parameter decays as $\phi \sim t^{-\delta}$, with $\delta = \beta$. In finite networks, on the other hand, the same mapping to a one-step process performed for the CP ensues from Eq. (22) (with the corresponding mapping $\lambda' = \lambda/2$), and therefore we expect for the TCP a FSS form given by Eqs. (3).

We finally note that Eqs. (21) and (22) lead to a stationary density of singly occupied nodes given by

$$\rho_k = \frac{1}{2} - \frac{\lambda k\phi}{4\langle k\rangle} + O[(k\phi)^2]. \tag{23}$$

Therefore, at criticality about 50% of the nodes belong to the backbone of singly occupied vertices through which the dynamics spreads. This result is verified with good accuracy in our simulation results, presented in Sec. VI.

V. SIMULATION METHODS

A. The quasistationary state method

In infinite systems, APTs are sharply defined. In finite systems, however, the absorbing state can be visited even in the supercritical phase due to stochastic fluctuations. The numerical exploration of APTs in this case is a subtle problem that must be handled with suitable simulation strategies. Here we investigate the stationary properties of the TCP using the quasistationary (QS) method [32], which has been successfully applied to determine with high accuracy the critical properties of the CP in SF networks [19,20]. In the QS method, every time the system tries to visit an absorbing configuration, the current configuration is replaced by one active state picked up randomly from the system history. The method is implemented by storing and constantly updating a list containing M active configurations previously visited by the dynamics. An update consists of randomly selecting a configuration in the list and replacing it with the present active configuration with a probability $p_r \Delta t$. After a relaxation time t_r, the QS probability $\bar{P}_n$, corresponding to states with n occupied vertices, is computed during an averaging interval t_a. All relevant QS quantities can be then determined from $\bar{P}_n$ as, for example, the density of active particles $\bar{\phi} = N^{-1}\sum_n n\bar{P}_n$ and the characteristic lifespan $\tau = 1/\bar{P}_1$ [19].

The networks used for simulations were generated using the uncorrelated configuration model (UCM) [41], with a minimum degree $m = 6$ and a hard cutoff $k_c = N^{1/2}$, which leads to the absence of the degree-degree correlations in large quenched SF networks [36] without self-connections or multiple connections. System sizes with up 1×10^7 nodes were used. Simulations were performed with fixed parameters $t_r = 4 \times 10^6$, $t_a = 4 \times 10^7$, and $M = 200$. The list with the system history must be updated according to the frequency with which the system tries to visit the absorbing state. The larger the lifespan τ the slower the list must be updated in the stationary state. In our simulations, we used $p_r = 10^{-3}$–10^{-2}, being the larger values used for the smaller network sizes.

B. Critical point determination: The moment ratio method

A key point in the numerical computation of critical exponents in any phase transition is the accurate determination of the critical point. The usual strategy to determine critical points in lattice models considers the search for pure power laws in plots of $\bar{\phi}$ or τ versus N [14]. This strategy, however, is not well suited to the presence of strong corrections to scaling, as expected for the TCP, given its relation with the CP. In Ref. [20], an alternative method was proposed, using the idea of size-independent critical moment ratios [42] in the form

$$M_{qs}^n = \frac{\langle \phi^n\rangle}{\langle \phi^q\rangle\langle \phi^s\rangle}, \quad q+s=n. \tag{24}$$

From the scaling form of $\bar{P}_n$, Eq. (2), we have

$$\langle n^k\rangle = \sum_{n=1}^{N} \frac{n^k}{\sqrt{\Omega}} f\left(\frac{n}{\sqrt{\Omega}}\right). \tag{25}$$

Defining $x = n/\sqrt{\Omega}$ with increments $\Delta x = 1/\sqrt{\Omega}$ we find

$$\langle n^k\rangle = \sqrt[k]{\Omega} \sum_{x=1/\sqrt{\Omega}}^{N/\Omega} x^k f(x)\Delta x \overset{N\to\infty}{=} a_k \sqrt[k]{\Omega}, \tag{26}$$

where $a_k = \int_0^\infty x^k f(x)dx$. Therefore, the asymptotic moment ratios at the mean-field level are size independent and given by $M_{qs}^n = a_n/a_q a_s$. One can thus estimate the critical point by taking advantage of this fact: Plotting the quantities M_n^{qs} as a function of λ for different values of N, the different curves will intersect at the critical point $\lambda = \lambda_c$, for all different network sizes [42]. Obviously, the validity of this scheme is conditioned to the scaling form of $\bar{P}_n$, which holds only for large systems, even at a mean-field level [19].

C. Check of numerical methods

In order to check the efficiency of our simulation and numerical methods, we have considered the TCP on top of annealed networks [18,43], in which all edges are rewired between any two dynamical steps while preserving the degree and degree correlations of each individual node. This procedure destroys all dynamical correlations and thus renders exact the predictions of HMF theory [6,18]. In practice, simulations on annealed networks are carried out in uncorrelated networks by selecting at random, every time that a node has to choose a nearest neighbor, a vertex of degree k in the whole network with a probability $kP(k)/\langle k\rangle$ [18]. In the following, we consider SF networks with a degree distribution $P(k) \sim k^{-\gamma}$ and $\gamma > 2$.

The HMF theory discussed in Sec. IV B predicts a FSS explicitly depending on the factor $g = \langle k^2\rangle/\langle k\rangle^2$ that, for SF networks with $2 < \gamma < 3$, behaves as $g \simeq \text{const} \times [1 - \xi^{3-\gamma} + 2\xi^{\gamma-2}\cdots]k_c^{3-\gamma}$, where $\xi = k_0/k_c$. So, even in annealed networks the FSS is ruled by strong corrections, especially for $\gamma \approx 3$ and $\gamma \approx 2$ when they become logarithmic. However, since HMF theory is exact in this case, the critical point must be $\lambda_c = 2$. We have checked that the moment ratio method precisely recovers this theoretical expectation, with all moment ratios, for different values of q and s and different network sizes, intersecting at $\lambda_c = 2$ for any value of γ.

Figure 1 shows the QS density and characteristic lifespan for critical TCP on annealed networks with degree exponents $\gamma = 2.25$ and $\gamma = 3.25$. The dependence of these quantities with the system size neatly deviates from the pure power law at criticality given by Eq. (5). This is, however, a simple finite-size effect; when the full factor g is explicitly included, we obtain a perfect agreement with HMF exponents $\bar{\phi} \sim (gN)^{-S_\nu}$ and $\tau \sim (N/g)^{S_\alpha}$ with $S_\nu = S_\alpha = 1/2$. The exponents obtained by means of linear regressions are $S_\nu = 0.498(3)$ and $0.502(3)$ while $S_\alpha = 0.499(2)$ and $0.498(2)$ for $\gamma = 2.25$ and 3.25, respectively.

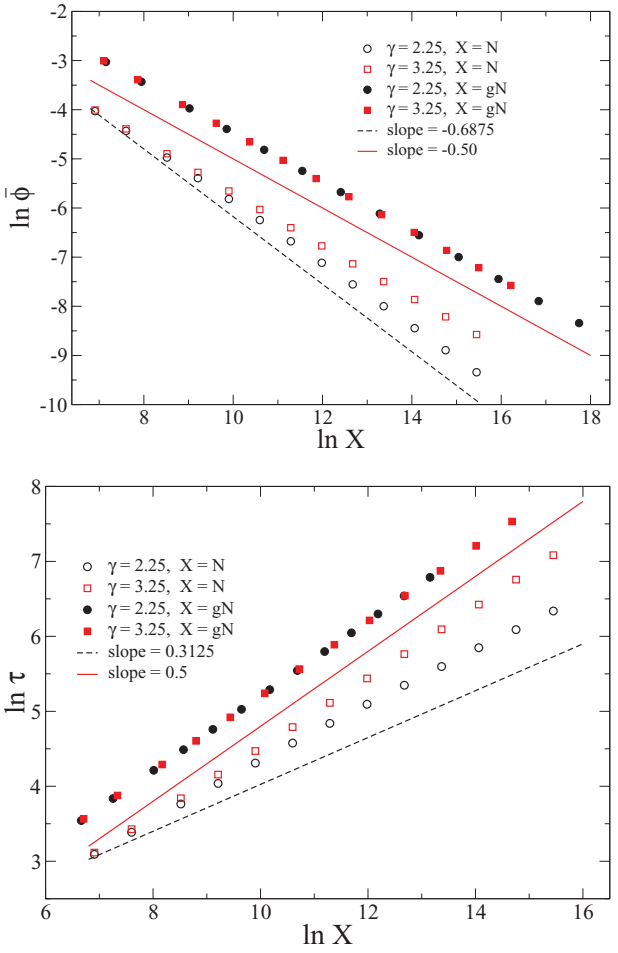

FIG. 1. (Color online) Finite-size scaling of the critical density (top) and characteristic lifespan (bottom) for the TCP on annealed SF networks. Symbols represent simulations; dashed lines are the scaling as a function of N expected from Eq. (5) for $\gamma = 2.25$; solid lines are the HMF theory predictions for $\gamma > 3$, Eq. (5), or for all γ when taking into account the full g dependence, Eq. (3). Solid symbols were shifted upwards to improve visibility.

VI. TCP ON QUENCHED NETWORKS

The excellent agreement between HMF and QS simulations on annealed networks is expected since the central MF hypotheses are fulfilled: absence of dynamical correlations and a distance between nodes $\ell \equiv 1$ [44], implying the exactness of the one-site approximation. In real (quenched) networks, whose edges are frozen and do not change in time, we usually still have the small-world property, but dynamical correlations are unavoidably present. An additional feature of TCP is that activity spreads through the backbone of occupied vertices. So, a necessary condition for the maintenance of activity is the existence of a giant component (GC) of connected vertices in the backbone [5]. This component is present in our simulations as discussed in the end of this section.

An important issue in the simulations is that, in opposition to the standard CP on quenched networks [20], the relaxation of TCP in SF networks depends on initial conditions. Figure 2 shows the critical relaxation in a quenched SF network ($\gamma = 2.75$) for two initial conditions. A fully active initial condition leads to a metastable phase where the system gets stuck into a pseudostationary state of very low density. After a transient, which can be very long for large sizes, the system evolves towards the real QS state. However, if we start with an initial condition having a small fraction of active vertices and the remaining ones occupied by a single particle, the metastable phase disappears and the system goes directly to the real QS state. This dependence on the initial condition is easily understood by considering that, in the early steps of a simulation with a fully active initial condition, annihilation events are predominant due to the lack of free space to create new particles. These annihilation events fragment the backbone into several small components and activity cannot spread until the backbone is regenerated, after a very large transient.

We thus choose to start with a 2% initial density of active vertices in all simulations reported in the following. Notice that the density of singly occupied nodes goes quickly to values very close to $1/2$ as shown in the inset of Fig. 2, but the final quasistationary state takes much longer in consonance with the quasistatic approximation used in HMF calculations of Sec. IV B.

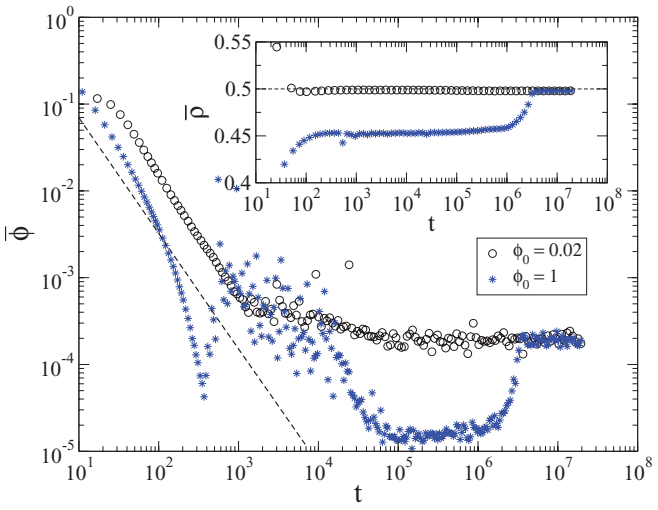

FIG. 2. (Color online) Critical relaxation of the density of active vertices for QS simulation of TCP on quenched SF networks with $\gamma = 2.75$ and size $N = 1.28 \times 10^6$. Two initial conditions are reported: fully active network (stars) and 2% of randomly distributed active vertices (circles). The dashed line is the power law decay $\phi \sim t^{-4/3}$ predicted by HMF theory. Inset: Critical relaxation of the density of singly occupied vertices in a semilogarithmic scale. The horizontal line indicates the density $\rho = 1/2$ predicted by the HMF theory, Eq. (23).

Critical points were determined using the moment ratio method described in Sec. V C. Figure 3 shows third and fourth order moment ratios against creation rates for networks of different sizes and degree exponents. All curves intersect closely at the same point yielding the critical points and moment ratio values shown in Table I. These moment ratio values are noticeably in good agreement with those obtained for CP simulations on the same kind of networks [20]. Notice also that the critical points are larger than the HMF prediction

TABLE I. Critical points and moment ratios for TCP on quenched SF networks.

γ	λ_c	M_{11}^2	M_{21}^3	M_{22}^4
2.50	2.1280(5)	1.87(2)	2.65(2)	4.73(5)
2.75	2.1661(2)	1.790(6)	2.43(3)	4.15(9)
3.25	2.2229(1)	1.712(8)	2.27(1)	3.71(4)

$\lambda_c = 2$, independently of γ. A satisfactory agreement between the homogeneous pair approximation value for the critical point, Eq. (17), and the QS simulations can be observed, however (see Fig. 4), again in conformity with the results for the CP on quenched networks [20,39].

Now in possession of accurate estimates of the critical points, we can check the validity of HMF critical exponents. Figure 5 shows the QS density and characteristic time for $\gamma = 2.50$ around the estimated critical point. Performing power law regression of these quantities as a function of N, a very good agreement with HMF exponents in Eq. (5) is found, as shown in Table II. Using the full anomalous FSS predicted by HMF theory, performing power law regressions of the form $\bar{\phi} \sim (Ng)^{-S_\nu}$ and $\tau \sim (N/g)^{S_\alpha}$, all numerically obtained exponents are in very good agreement with the HMF result $S_\alpha = S_\nu = 1/2$. The agreement of simulations with HMF theory extends to all the values of γ considered, as shown in Table II.

We have finally investigated the backbone of the network used for the spreading of activity, which is defined as the largest connected cluster (giant component) of vertices having at least one particle. Figure 6 shows the average fraction of vertices belonging to the backbone in the critical TCP against network size. The size of the GC corresponding to a random dilution of 50% is also shown for the sake of comparison. It is well known that SF networks are resilient to random removal of nodes, such that a giant component persists even if a finite

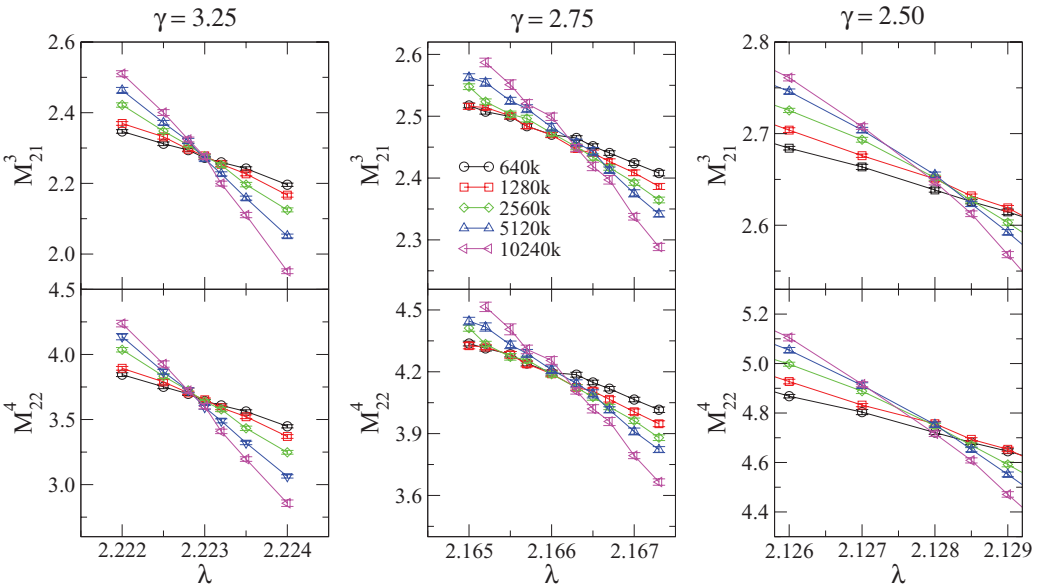

FIG. 3. (Color online) Moment ratios against creation rate of the TCP on quenched SF networks with different values of γ, for several system sizes. For the sake of comparison, all plots have the same horizontal range.

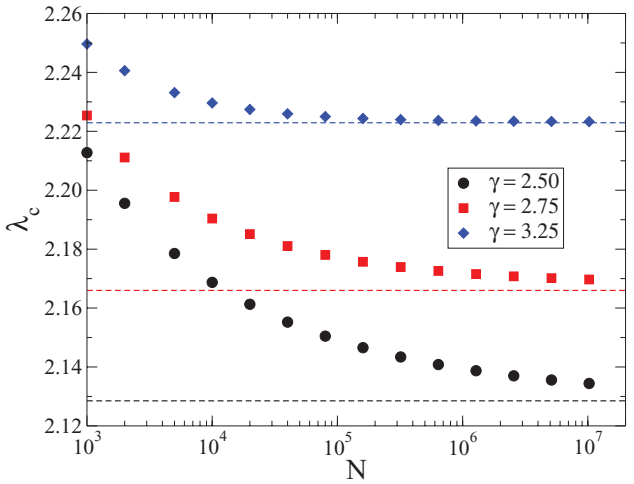

FIG. 4. (Color online) Comparison between critical points obtained in a homogeneous pair approximation (symbols) and QS simulations (lines) of the TCP on quenched SF networks. HPA results correspond to Eq. (17) with the coordination q replaced by the average degree of the network.

fraction of the nodes is removed [11,12]. A random dilution of 50% of the nodes in UCM networks leads to GCs containing almost the totality of the nondiluted nodes (Fig. 6). The critical TCP dynamics generates a backbone with a similar fraction of vertices. The second largest connected cluster contains just a few nodes (typically three or four for a network size $N \simeq 1 \times 10^7$) and, therefore, the activity in regions disconnected from the backbone is negligible.

Noticeably, while random dilution and critical TCP on homogeneous and large networks ($\gamma = 3.25$) generate GCs that do not vary with network size, in the heterogeneous case we have a slow (sublogarithmic) increase, which is more apparent the smaller the value of γ. This dependence of the

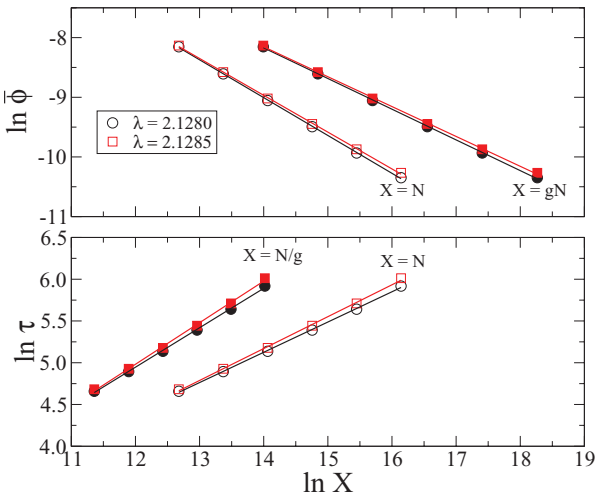

FIG. 5. (Color online) Finite size scaling of the QS density $\bar{\phi}$ and characteristic time τ around the critical point for quenched SF networks with $\gamma = 2.50$. Solid lines are linear regressions used to estimate the scaling exponents. Open symbols refer to plots against size N while solid symbols refer to the plots against size rescaled by the factor $g = \langle k^2 \rangle / \langle k \rangle^2$.

TABLE II. Critical exponents for TCP on quenched SF networks. HMF exponents $\hat{\nu}_{\rm HMF}$ and $\hat{\alpha}_{\rm HMF}$, as given by Eq. (5), are included for comparison.

γ	$\hat{\nu}$	$\hat{\nu}_{\rm HMF}$	S_ν	$\hat{\alpha}$	$\hat{\alpha}_{\rm HMF}$	S_α
2.50	0.62(1)	0.625	0.51(1)	0.37(1)	0.375	0.48(1)
2.75	0.57(1)	0.5625	0.496(8)	0.42(1)	0.4375	0.50(1)
3.25	0.50(1)	0.500	0.48(1)	0.49(2)	0.500	0.51(2)

backbone size with N is, however, so slow (e.g., a relative variation of around 0.5% when size increases from 1×10^3 to 1×10^7 for $\gamma = 2.50$) that its effect is essentially negligible, as can be seen from the excellent agreement with HMF theory shown by numerical simulations.

VII. DISCUSSION

In the present work, we have studied the absorbing-state phase transition of a TCP in networks. The model, possessing infinitely many absorbing configurations in the thermodynamic limit, is analogous to the pair contact process [24] with a relaxation of the fermionic constraint: Up to two particles can occupy a vertex but only the particles in doubly occupied vertices react (annihilate or create a new particle in a nearest neighbor).

Applying the standard heterogeneous mean-field theory and extensive large-scale numerical simulations based on the quasistationary state method, we have shown that the critical behavior of the TCP is exactly the same as the standard CP and, therefore, that both models belong to the so-called CP-HMF universality class in networks, which is defined, at the FSS level, by the set of exponents given by Eq. (5). At this respect, the apparent non-mean-field exponents reported in Ref. [29] for the related pair contact process, a fermionic counterpart of the TCP, can probably be attributed to the networks sizes considered in that work ($N \lesssim 1 \times 10^4$), much smaller than the largest system sizes ($N \sim 1 \times 10^7$) that we attain here.

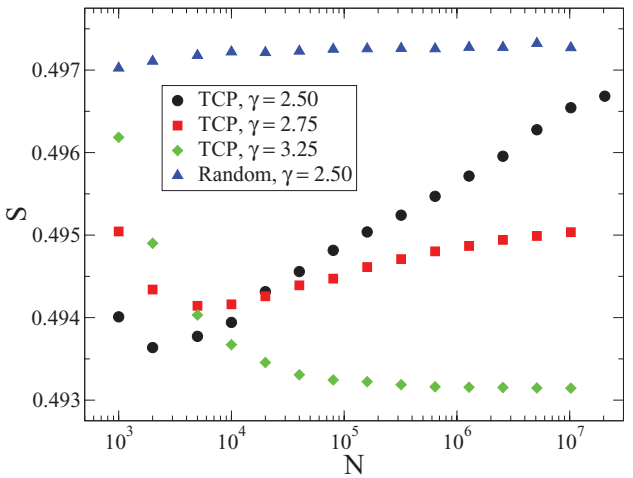

FIG. 6. (Color online) Average size of the giant component against network size obtained with the TCP dynamics or a random dilution of 50% of the vertices. The random dilution for other γ values have the same behavior of $\gamma = 2.50$.

The CP-HMF universality class studied here can be conjectured to include other CP-like models with a finite or infinite number of absorbing states. However, its status is not as robust as in lattices, since in networks microscopic details of the models can be enhanced due to heterogeneity. For example, the susceptible-infected-susceptible (SIS) epidemic model [45] is a variation of the CP in which a vertex produces activity in all its neighbors with the same strength, while in the CP the activity production of a vertex is equally divided among all neighbors [factor $1/k'$ in Eq. (20)]. According to the Janssen-Grassberger conjecture [46,47], the universality class of CP and SIS should be the same, and in fact both models belong to the DP universality class in homogeneous lattices. In complex networks, however, heterogeneity strongly affects both models and it renders the SIS with critical exponents at the HMF level which are different from the CP [45]. Moreover, the SIS can be shown to exhibit a vanishing critical point in the thermodynamical limit if the maximal connectivity is unbounded [48,49].

We can thus conjecture a splitting of universality classes comprising at least a CP-HMF and a SIS-HMF class, which are independent of the number of absorbing states (as proved in the SIS case by the study of the forest-fire model [28]) but depends on the way in which activity spreads over nearest neighbors. Further work should be devoted to the study of this universality class splitting in complex networks.

ACKNOWLEDGMENTS

This work was partially supported by the Brazilian agencies CNPq, FAPEMIG, and CAPES. R.P.-S. acknowledges financial support from the Spanish MEC, under Project No. FIS2010-21781-C02-01; the Junta de Andalucía, under Project No. P09-FQM4682; ICREA Academia, funded by the Generalitat de Catalunya; partial support by the NSF under Grant No. PHY1066293; and the hospitality of the Aspen Center for Physics, Colorado, where part of this work was performed.

[1] B. D. Hugues, *Random Walks and Random Environments, Vol. II, Random Environments* (Clarendon Press, Oxford, 1996).
[2] D. Ben-Avraham and S. Havlin, *Diffusion and Reactions in Fractals and Disordered Systems* (Cambridge University Press, Cambridge, 2000).
[3] R. Albert and A.-L. Barabási, Rev. Mod. Phys. **74**, 47 (2002).
[4] S. N. Dorogovtsev and J. F. F. Mendes, *Evolution of Networks: From Biological Nets to the Internet and WWW* (Oxford University Press, Oxford, 2003).
[5] M. Newman, *Networks: An Introduction* (Oxford University Press, Oxford, 2010).
[6] S. N. Dorogovtsev, A. V. Goltsev, and J. F. F. Mendes, Rev. Mod. Phys. **80**, 1275 (2008).
[7] A. Barrat, M. Barthélemy, and A. Vespignani, *Dynamical Processes on Complex Networks* (Cambridge University Press, Cambridge, 2008).
[8] R. Pastor-Satorras and A. Vespignani, Phys. Rev. Lett. **86**, 3200 (2001).
[9] R. M. May and A. L. Lloyd, Phys. Rev. E **64**, 066112 (2001).
[10] M. E. J. Newman, Phys. Rev. E **66**, 016128 (2002).
[11] R. Cohen, K. Erez, D. ben-Avraham, and S. Havlin, Phys. Rev. Lett. **85**, 4626 (2000).
[12] D. S. Callaway, M. E. J. Newman, S. H. Strogatz, and D. J. Watts, Phys. Rev. Lett. **85**, 5468 (2000).
[13] A. Arenas, A. Diaz-Guilera, J. Kurths, Y. Moreno, and C. Zhou, Phys. Rep. **469**, 93 (2008).
[14] J. Marro and R. Dickman, *Nonequilibrium Phase Transitions in Lattice Models* (Cambridge University Press, Cambridge, 1999).
[15] M. Henkel, H. Hinrichsen, and S. Lübeck, *Non-equilibrium Phase Transition: Absorbing Phase Transitions* (Springer-Verlag, Amsterdam, 2008).
[16] T. E. Harris, Ann. Probab. **2**, 969 (1974).
[17] C. Castellano and R. Pastor-Satorras, Phys. Rev. Lett. **100**, 148701 (2008).
[18] M. Boguñá, C. Castellano, and R. Pastor-Satorras, Phys. Rev. E **79**, 036110 (2009).
[19] S. C. Ferreira, R. S. Ferreira, and R. Pastor-Satorras, Phys. Rev. E **83**, 066113 (2011).
[20] S. C. Ferreira, R. S. Ferreira, C. Castellano, and R. Pastor-Satorras, Phys. Rev. E **84**, 066102 (2011).
[21] F. van Wijland, Braz. J. Phys. **33**, 551 (2003).
[22] B. Drossel and F. Schwabl, Phys. Rev. Lett. **69**, 1629 (1992).
[23] R. Dickman, A. Vespignani, and S. Zapperi, Phys. Rev. E **57**, 5095 (1998).
[24] I. Jensen, Phys. Rev. Lett. **70**, 1465 (1993).
[25] K.-I. Goh, D.-S. Lee, B. Kahng, and D. Kim, Phys. Rev. Lett. **91**, 148701 (2003).
[26] D. O. Cajueiro and R. Andrade, Eur. Phys. J. B **77**, 291 (2010).
[27] D.-S. Lee, K.-I. Goh, B. Kahng, and D. Kim, Physica A **338**, 84 (2004).
[28] J.-D. Bancal and R. Pastor-Satorras, Eur. Phys. J. B **76**, 109 (2010).
[29] H. Da-Yin and W. Lie-Yan, Chin. Phys. Lett. **27**, 098901 (2010).
[30] Edited by J. L. Cardy, *Finite Size Scaling*, Vol. 2 (North-Holland, Amsterdam, 1988).
[31] A. Vespignani, Nat. Phys. **8**, 32 (2012).
[32] M. M. de Oliveira and R. Dickman, Phys. Rev. E **71**, 016129 (2005).
[33] C. Castellano and R. Pastor-Satorras, Phys. Rev. Lett. **96**, 038701 (2006).
[34] R. Pastor-Satorras, A. Vázquez, and A. Vespignani, Phys. Rev. Lett. **87**, 258701 (2001).
[35] J. D. Noh and H. Park, Phys. Rev. E **79**, 056115 (2009).
[36] M. Boguñá, R. Pastor-Satorras, and A. Vespignani, Eur. Phys. J. B **38**, 205 (2004).
[37] J. Kockelkoren and H. Chaté, Phys. Rev. Lett. **90**, 125701 (2003).
[38] D. ben-Avraham and J. Köhler, Phys. Rev. A **45**, 8358 (1992).
[39] M. A. Muñoz, R. Juhász, C. Castellano, and G. Ódor, Phys. Rev. Lett. **105**, 128701 (2010).
[40] M. Catanzaro, M. Boguñá, and R. Pastor-Satorras, Phys. Rev. E **71**, 056104 (2005).

[41] M. Catanzaro, M. Boguñá, and R. Pastor-Satorras, Phys. Rev. E **71**, 027103 (2005).
[42] D. Landau and K. Binder, *A Guide to Monte Carlo Simulations in Statistical Physics*, 3rd ed. (Cambridge University Press, New York, 2009).
[43] D. Stauffer and M. Sahimi, Phys. Rev. E **72**, 046128 (2005).
[44] In an annealed substrate a given node interacts with any node of the network including itself due to the connectivity rewiring.
[45] R. Pastor-Satorras and A. Vespignani, Phys. Rev. E **63**, 066117 (2001).
[46] H. K. Janssen, Z. Phys. B: Condens. Matter **42**, 151 (1981).
[47] P. Grassberger, Z. Phys. B: Condens. Matter **47**, 365 (1982).
[48] C. Castellano and R. Pastor-Satorras, Phys. Rev. Lett. **105**, 218701 (2010).
[49] S. C. Ferreira, C. Castellano, and R. Pastor-Satorras, Phys. Rev. E **86**, 041125 (2012).